Journal of Macromolecular Science, Part A
Publication details, including instructions for authors and subscription information:
http://www.informaworld.com/smpp/title~content=t713597274

Syntheses and Characterization of 4-Octyloxybenzyl Substituted Diketopyrrolopyrrole-based Red Emitting Copolymers with Low Turn-on Voltage

Yanbin Xu[a]; Yi Jin[a]; Junbiao Peng[b]; Baozheng Wang[b]; Derong Cao[a]
[a] School of Chemistry and Chemical Engineering, South China University of Technology, Guangzhou, China [b] Institute of Polymer Optoelectronic Materials and Devices, South China University of Technology, Guangzhou, China

To cite this Article Xu, Yanbin , Jin, Yi , Peng, Junbiao , Wang, Baozheng and Cao, Derong(2010) 'Syntheses and Characterization of 4-Octyloxybenzyl Substituted Diketopyrrolopyrrole-based Red Emitting Copolymers with Low Turn-on Voltage', Journal of Macromolecular Science, Part A, 47: 11, 1059 — 1068

To link to this Article: DOI: 10.1080/10601325.2010.511091

URL: http://dx.doi.org/10.1080/10601325.2010.511091

Journal of Macromolecular Science, Part A: Pure and Applied Chemistry (2010) **47**, 1059–1068

ISSN: 1060-1325 print / 1520-5738 online
DOI: 10.1080/10601325.2010.511091

Syntheses and Characterization of 4-Octyloxybenzyl Substituted Diketopyrrolopyrrole-based Red Emitting Copolymers with Low Turn-on Voltage

YANBIN XU[1], YI JIN[1], JUNBIAO PENG[2], BAOZHENG WANG[2] and DERONG CAO[1,*]

[1]*School of Chemistry and Chemical Engineering, South China University of Technology, Guangzhou, China*
[2]*Institute of Polymer Optoelectronic Materials and Devices, South China University of Technology, Guangzhou, China*

Received, Accepted June 2010

Two novel diketopyrrolopyrrole-based alternating copolymers, poly(2,7-(9,9-diethyl)-fluorenylvinylene-*alt*-2,5-bis(4′-octyloxyphenylmethyl)-3,6-bis(4-vinylenephenyl)pyrrolo[3,4-c]pyrrole-1,4-dione) (**P1**) and poly(1,4-(2,5-dioctyl- oxy)-phenylenevinylene-*alt*-2,5-bis(4′-octyloxyphenylmethyl)-3,6-bis(4-vinylenephenyl)pyrrolo[3,4-c]pyrrole-1,4-dione) (**P2**) were synthesized through Wittig polycondensation in good yields. **P1** and **P2** were characterized by NMR, FT-IR, UV-Vis, photoluminescence (PL) and electroluminescence (EL). EL devices with ITO/PEDOT/polymer/CsF/Al exhibited red-emitting light with the maximum EL wavelength at 620 nm and 682 nm. The results show that PL quantum yield of the polymers in thin film can be improved through *N*-alkylation of diketopyrrolopyrrole (DPP) with bulky substituent. EL performance of **P2** was better than **P1**, which might be due to 1,4-dioctyloxybenzene of **P2** enhancing the hole-transporting to make more charge balance. EL devices of **P1** and **P2** possessed low turn on voltage (2.4 V and 2.1 V, respectively), which was an advantage for PLED.

Keywords: Diketopyrrolopyrrole, light-emitting diodes, conjugated polymer, Wittig polymerization

1 Introduction

Since electroluminescence (EL) in conjugated polymers was first reported in poly(*para*-phenylene vinylene) in 1990 (1), considerable efforts have been devoted to developing conjugated materials as the active units in light-emitting devices for use in display applications (2). Polyfluorene has been extensively studied owing to its distinct blue electroluminescence and relatively high carrier mobility. The development of fluorene-containing copolymers whose colors span the entire visible range has been actively investigated. However, the development of efficient fluorene-based copolymers with red emission for polymer light emitting diodes (PLED) applications remains a challenging task (3, 4) because red chromophores are prone to aggregation in the solid state and are highly susceptible to concentration quenching (5). Moreover, available red-emitting polyfluorene derivatives are still relatively scarce, therefore further improvements are necessary.

Diketopyrrolopyrrole (DPP) derivatives represent high stability and photoelectric properties. They have been used in preparation of photorefractive (6), solid state-dye laser (7), photovoltaic cells (8–10), field-effect transistors (FETs) (11). They are potential red-emitting materials for PLED (12–14).

Most DPP-based polymers have excellent photoluminescence (PL) in solution, which have been studied wildly (15–17). However, the studies of DPP-based polymers in solid and especially in PLED are limited. DPP molecule is virtually planar (18) and includes a conjugated bicyclic structure, which leads to strong π-π interactions (19,20) and aggregation in solid state (21). Generally, this aggregation leads to photoluminescence quenching (22), and is a disadvantage for the electroluminescence's (EL) performance (2). *N*-alkylation of lactam units of DPP was used to increase its solubility (12). The allylic chains are nearly perpendicular to the heterocycle (23). This is benefit to reduce the aggregation, because bulky side group can be used to reduce the aggregation, which results in more spaced packing and correspondingly leads to highly luminescence in powders and films (24).

Compared with polyflourene (HOMO level is about −5.8 eV) (25), polyfluorenevinylene (PFV) possesses a higher HOMO level (−5.5 eV) (26) which is closer to the

---

*Address correspondence to: D. Cao, School of Chemistry and Chemical Engineering, South China University of Technology, Guangzhou 510640, China. Tel: +86-20-87110245; Fax: +86-20-87110245; E-mail: drcao@scut.edu.cn

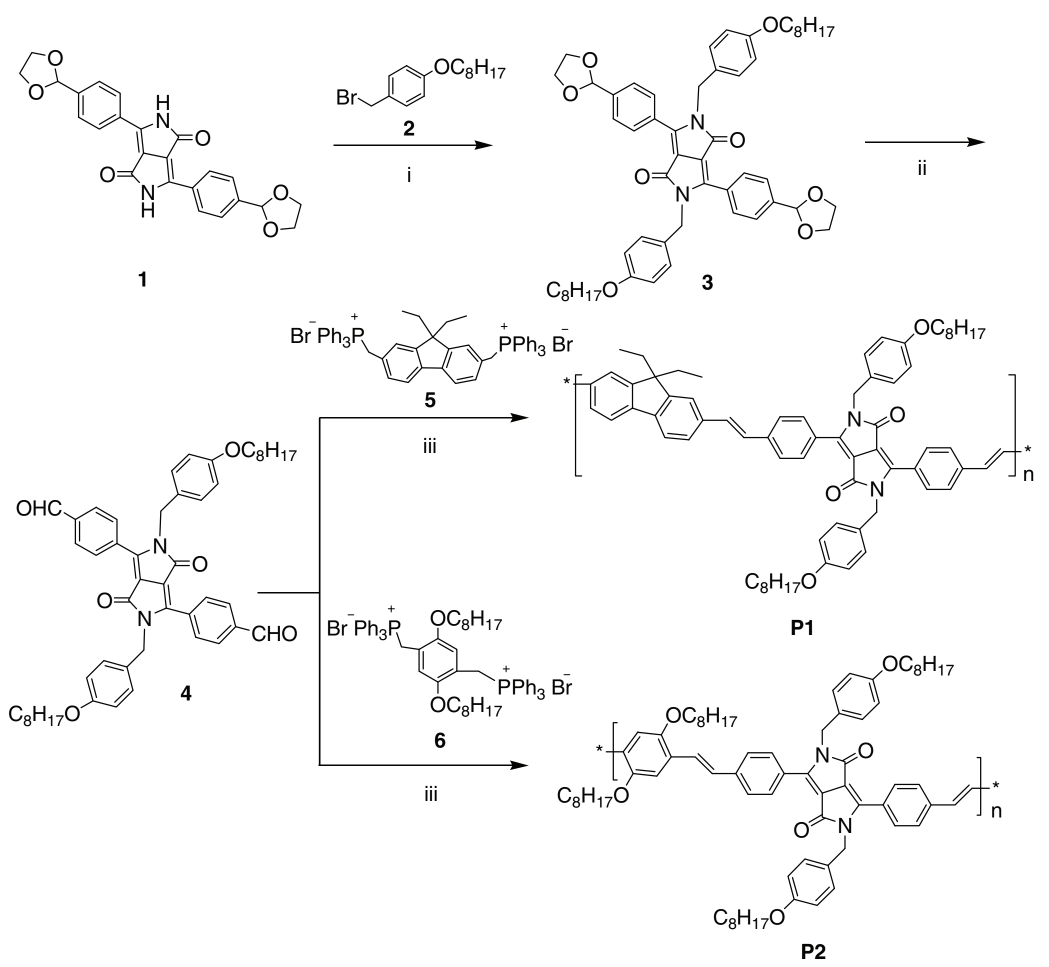

^{a}Reagents and conditions: (i) potassium tert-butanolate, NMP, N_2, rt, 24 h, yield 29%; (ii) 2M HCl, THF, 60°C 2 h, 91%; (iii) sodium *tert*-butanolate, N_2, rt, 24 h.

Sch. 1. Synthetic route of **P1** and **P2**^{a}.

work function of ITO/PEDOT (-5.0 eV). Moreover, some alkoxy-substituted PPVs possess an even higher HOMO level, for example, poly[2-methoxy-5-(2-ethylhexyloxy)-1,4-phenylenevinylene] (MEH-PPV) (-5.1 eV) (25). A low energy barrier between the emitting layer and electrode is helpful to charge carrier injection. In this paper, two DPP-based polymers (Sch. 1) named **P1** and **P2** were prepared by Wittig polymerization. 4-Octyloxybenzyl was used as a substituent in *N*-alkylation. Compared with alkyl chain, this bulky side group might further reduce the aggregation between DPP units and polymer chains. Both polymers were used as an active layer in light emitting diodes of ITO/PEDOT/polymer/CsF/Al. The PL and EL properties of the polymers were investigated and discussed.

2 Experimental

2.1 Measurement and Characterization

NMR (^{1}H and ^{13}C) spectra were collected on a Bruker DRX 400 spectrometer in $CDCl_3$ with tetramethylsilane as inner reference. Fourier transform infrared (FTIR) spectra were recorded on an RFX-65A (Analect Co.) spectrometer with KBr pellets. Mass spectrum was recorded on a Bruker Esquire HCT PLUS. The number-average molecular weight (M_n) and weight-average molecular weights (M_w) were determined by Waters GPC 515–410 in tetrahydrofuran (THF) with a calibration curve of polystyrene standards. Thermogravimetric analysis (TGA) was conducted on a Netzsch STA449C TGA instrument at heating rate of 10°C/min and N_2 flow rate of 20 mL/min. Differential scanning calorimetry (DSC) measurements was performed on a Diamond DSC instrument under N_2 at a heating rate of 10°C/min. Elemental analysis was performed with a Vario EL III instrument. Cyclic voltammetry (CV) was carried out on an EG&G model 283 computer-controlled potential/galvanostat (Princeton Applied Research) with platinum electrodes at a scanning rate of 50 mV/s against a calomel reference electrode with a nitrogen-saturated solution of 0.1 M tetrabutylammonium hexafluorophosphate (Bu_4NPF_6) in anhydrous spectrum-grade acetonitrile (CH_3CN). Ultraviolet-visible (UV-vis) absorption spectra were recorded on an HP 4803 instrument. Photoluminescence (PL) spectra were recorded on an Instaspec IV CCD spectrophotometer (Oriel Co.). Current-voltage characteristics were recorded with a Keithley 236 computerized source meter. Solid PL quantum yields were determined in an IS080 integrating sphere (Labsphere) with 325 nm excitation of a HeCd laser (MElls Griot). Solution PL quantum yields were measured in chloroform with an excitation wavelength of 400 nm, and the values were calculated by comparing with Rhodamine 6G in water ($\Phi_f = 0.95$) according to the published literature (27).

2.2 Materials

Compound **1** (28), **5** (29), **6** (30), and 4-octyloxybenzyl alcohol (31) were synthesized according to the published literature; other chemicals were obtained from commercially available resources.

2.2.1. *3,6-Bis(4-formylphenyl)-2,5-bis(4-octyloxybenzyl) pyrrolo[3,4-c]pyrrole-1,4-dione (4)*

PBr_3 (1.0 ml) in 3 ml of CH_2Cl_2 was added dropwise to a solution of 4-octyloxybenzyl alcohol (5.90 g, 25 mmol) in 15 ml of CH_2Cl_2 at 0°C in 1 h, then the mixture was kept stirring for 2 h at 0°C and at room temperature for 1 h. The mixture was poured into water and extracted with 30 ml of CH_2Cl_2. The organic layer was washed with brine, $NaHCO_3$ (5%) and water, then dried over with anhydrous $MgSO_4$. The solvent was removed via rotatory evaporation to give 1-bromomethyl-4-octyloxy-benzene (**2**) which was used for the next step directly.

A mixture of 3,6-bis-(4-[1,3]dioxolan-2-yl-phenyl)-2,5-dihydro-pyrrolo[3,4- c]pyrrole-1,4-dione (**1**) (2.16 g, 5 mmol) and potassium *tert*-butanolate (1.68 g, 15 mmol) in 50 ml of 1-methyl-2-pyrrolidinone (NMP) was stirred for 1 h under N_2, then 1-bromomethyl-4-octyloxy-benzene (**2**) was added dropwise and the mixture was kept stirring for further 24 h. The mixture was diluted with CH_2Cl_2 and filtrated. The filtrate was washed with brine and water, then dried over with anhydrous $MgSO_4$ and the solvent was removed via rotatory evaporation. The raw product was purified via gel column chromatography with CH_2Cl_2 and petroleum ether as the eluent to give 3,6-bis-(4-[1,3]dioxolan-2-yl-phenyl)-2,5-bis-(4-octyloxy-benzyl)-2,5-dihydro- pyrrolo[3,4-c]pyrrole-1,4-dione (**3**) as glassy yellow crystal (1.25 g, 29%), m.p. 180~181°C.

THF (15 ml) and HCl (6 ml, 2M) were added to the above residue of **3** and was stirred for 2 h at 60°C. The mixture was cooled to room temperature and poured into ice water. Red precipitate was collected and recrystallized from CH_2Cl_2 and methanol to give **4** as red crystal (0.90 g, 91% yield), m.p. 175~176°C. ^{1}H-NMR (400 MHz, $CDCl_3$) (δ/ppm): 0.86 (t, 6H, $J = 6.8$ Hz), 1.25~1.30 (m, 16H), 1.39~1.41 (m, 4H), 1.71~1.75 (m, 4H), 3.88 (t, 4H, $J = 6.8$ Hz), 4.89 (s, 4H), 6.77~6.79 (d, 4H, $J = 8.8$ Hz), 7.01~7.03 (d, 4H, $J = 8.8$ Hz), 7.89~7.92 (d, 4H, $J = 8.4$ Hz), 7.94~7.96 (d, 4H, $J = 8.4$ Hz), 10.05 (s, 2H). ^{13}C-NMR (100 MHz, $CDCl_3$) (δ/ppm): 191.2, 162.4, 158.6 148.1 137.7 133.0, 129.9, 129.7, 128.6, 128.1, 114.8, 111.1, 68.0, 45.2, 31.8 29.3, 29.2, 29.2, 26.0, 22.6, 14.1. FTIR (KBr, cm^{-1}): 3064 (ν, Ar—H), 2920, 2849 (ν, CH_2), 2745, 1706 (ν, H—C=O), 1673 (ν, C=O), 1597, 1579, 1509, 1474 (ν, ArC=C), 1244, 1047 (ν, C—O—C), 837 (δ, Ar—H). MS (APCI): m/z 781 (MH^+, 100). Anal. Calcd for$C_{50}H_{56}N_2O_6$: C, 76.89; H, 7.23; N, 3.59. Found: C, 76.80, H, 7.55, N, 3.54.

2.2.2. *Poly(2,7-(9,9-diethyl)-fluorenylvinylene-alt-2,5-bis(4′-octyloxyphenyl-methyl)-3,6-bis(4-vinyl-enephenyl)pyrrolo[3,4-c]pyrrole-1,4-dione) (P1)*

Sodium *tert*-butanolate (2.4 ml, 0.26 mol/L in *tert*-butyl alcohol) was added dorpwise to the solution of **5** (0.279 g, 0.3 mmol) and **4** (0.236 g, 0.3 mmol) in 10 ml of chloroform in 1 h under N_2. The mixture was stirred at room temperature for 24 h. The mixture was slowly poured into 15 ml of methanol and the precipitate was dissolved in 3 ml of chloroform again, then poured into 20 ml of acetone. The turbid liquid was separated by using a centrifuge under 10000 r/min, and the solid was extracted with acetone in Soxhlet apparatus for 24 h to give **P1** as dark-red solid (0.178 g, 60% yield). ^{1}H-NMR (400 MHz, $CDCl_3$) (δ/ppm): 0.21~1.75 (m, 40H), 3.84~3.92 (d, 4H), 4.93 (s, 4H), 6.57~7.83 (m, 26H). FTIR (KBr, cm^{-1}): 3030 (ν, Ar—H), 2957, 2869 (ν, CH_3), 2924, 2852 (ν, CH_2), 1673 (ν, C=O), 1597, 1544, 1509, 1463 (ν, ArC=C), 1246, 1047 (ν, C—O—C), 825 (δ, Ar—H).

2.2.3. *Poly(1,4-(2,5-dioctyloxy)-phenylenevinylene-alt-2,5-bis(4′-octyloxyphenylmethyl-3,6-bis(4-vinyl-enephenyl)pyrrolo[3,4-c]pyrrole-1,4-dione) (P2)*

The synthesis of this polymer was accomplished using the same method as **P1** by using 2,5-dioctyloxy-benzene-1,4-bis(methyl-triphenyl-phosphonium bromide) (**6**) in place of **5**. **P2** was obtained as a purplish black solid (0.201 g, 60% yield). ^{1}H-NMR (400 MHz, $CDCl_3$) (δ/ppm): 0.82~1.89 (m, 60H), 3.57~3.64 (d, 2H), 3.90 (s, 4H), 4.00~4.07 (d, 2H), 4.88~4.94 (d, 4H), 6.58~7.81 (m, 22H). FTIR (KBr, cm^{-1}): 3041(ν, Ar—H), 2955 (ν, CH_3), 2924, 2854 (ν, CH_2),

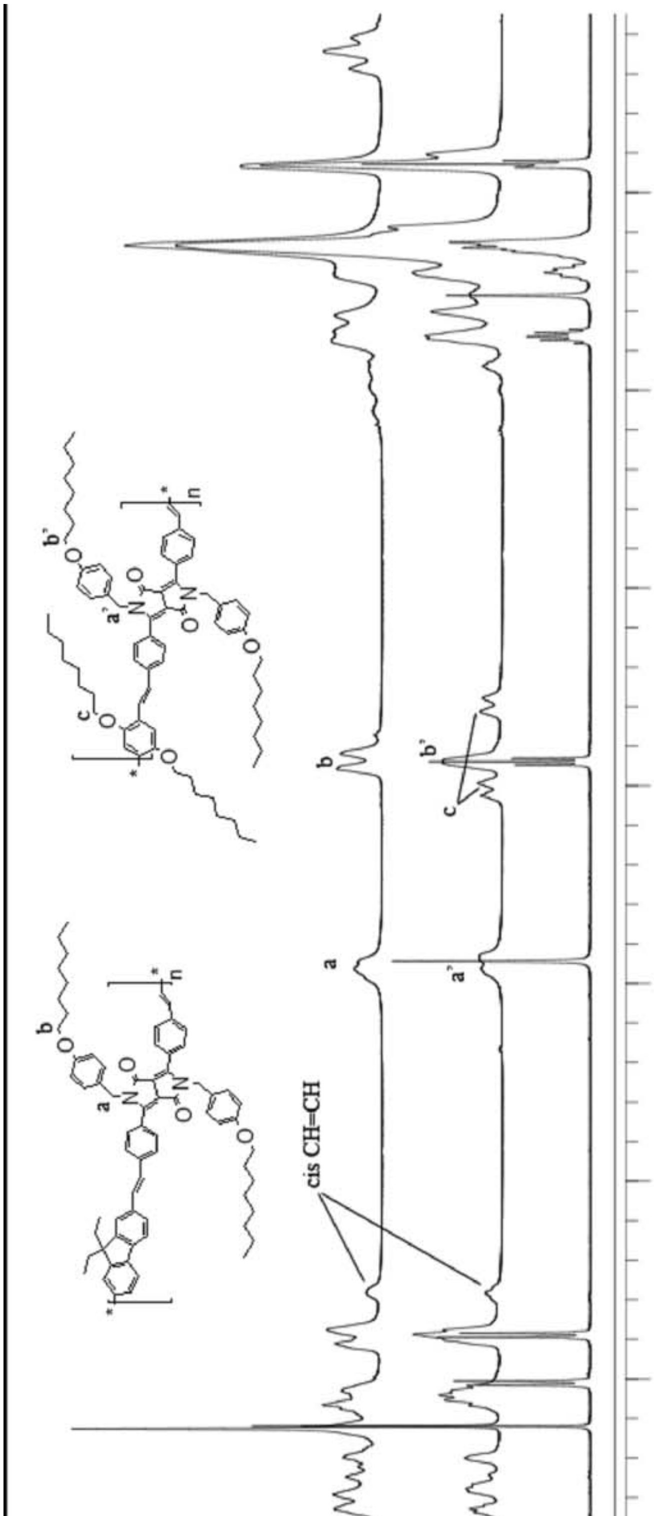

Fig. 1. ^{1}H-NMR spectra of **P1**, **P2** and compound **4**.

1673 (ν, C=O), 1599, 1542, 1513, 1467 (ν, ArC=C), 1246, 1074 (ν, C–O–C), 826 (δ, Ar–H).

2.3 Light-Emitting Diode (LED) Fabrication and Characterization

P1 and **P2** were dissolved in toluene and THF and filtered through a 0.45- μm filter. Patterned indium tin oxide (ITO) coated glass substrates were cleaned with acetone, detergent, distilled water, and 2-propanol and subsequently in an ultrasonic bath. After treatment with oxygen plasma, 40 nm of poly(3,4-ethylenedioxythiophene) (PEDOT) doped with poly(styrenesulfonic acid) (PSS; Batron-P 4083, Bayer AG) was spin-coated onto the ITO substrate, and this was followed by drying in a vacuum oven. A thin film of **P1** or **P2** was coated onto the anode via spin casting inside a drybox. The film thickness of the active layers was 70 nm, as measured with Alfa Step 500 surface profiler (Tencor). A thin layer of CsF (1.5 nm) and subsequently 140 nm layers of Al were vacuum-evaporated subsequently on the top of an EL polymer layer under a vacuum of 1×10^{-4} Pa.

3 Results and Discussions

3.1 Synthesis and Characterization

The synthetic route of the monomers and the polymers is outlined in Scheme 1. Monomer **4** was prepared in a two-step process: substitution of the lactam NH groups of the DPP units and hydrolysis. In order to prepare soluble DPP-polymers and to reduce film state aggregation of the polymers, 4-octyloxybenzyl unit was introduced. **P1** and **P2** were synthesized through Wittig polycondensation as it's a moderate and catalyst free reaction, and purified by centrifugal separation and extraction with the yield of 60%.

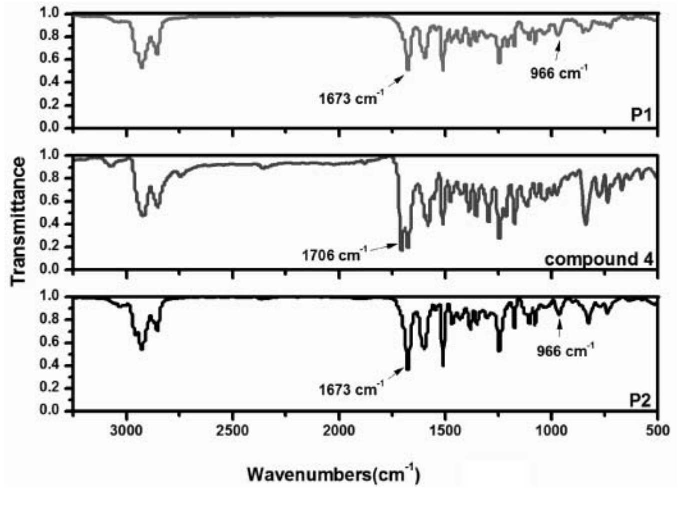

Fig. 2. FT-IR spectra of **P1, P2** and compound **4**.

Table 1. Molecular weight and thermal properties of **P1** and **P2**

Polymer	M_w	M_n	T_d (°C)	T_g(°C)
P1	27316	10632	381	126
P2	49885	12032	387	70

The polymer chemical structures were verified by ^{1}H-NMR and FTIR spectroscopy. From the ^{1}H-NMR spectra (Fig. 1), the singles of the methylene group adjacent to the lactam N atom of **P1** and **P2** appeared at 4.93 ppm and 4.88~4.94 ppm, respectively. A characteristic signal of the α-CH_2 groups directly attached to O atom in DPP unit appeared at 3.84~3.92 ppm and 3.89~3.90 ppm, respectively. Because a typical Wittig reaction yielded a mixture of cis/trans olefin geometries (32), the signal of α-CH_2 groups directly attached to O atom in **P2** main chain appeared at 3.57~3.64 ppm and 4.00~4.07 ppm with the ratio of 1 to 1, which were related to cis- and trans-olefins, respectively (32). In addition, the peaks at 6.5 ppm were assigned to the cis-vinylic linkages of both polymers. FT-IR spectra (Fig. 2) show that the typical C=O stretching absorption of alkylated lactam group of the monomer and polymers was at 1673 cm^{-1}, and the C=O stretching absorption of aldehyde group of the monomer was at 1706 cm^{-1}. The peak at 966 cm^{-1} was attributed to the trans-olefins of the two polymers (33).

The molecular weights (Table 1) were determined by gel permeation chromatography (GPC) with polystyrene as the standard and THF as the eluent. The $M_n$values of **P1** and **P2** were 10632 and 12032, and the two polymers possess similar degrees of polymerization (10.6 and 10.8). **P1** and **P2** were soluble in conventional organic solvents, such as chloroform, toluene, tetrahydrofuran (THF).

P1 and P2 possessed good thermal stability (Table 1) which was valuable for their application in PLED as there was a lot of heat produced during operation. The glass transition temperature (T_g) of **P1** was higher than that of **P2**. This suggested that **P1**'s backbone should be of higher rigidity than **P2**'s (34, 35).

3.2 Photophysical Properties

The photophysical characteristics of copolymers are summarized in Table 2. Figure 4 presents the absorption spectra of polymers in dilute $CHCl_3$ solution (10^{-5} M). The maximum absorptions (λ_{max}) of **P1** and **P2** were at 520 nm and

Table 2. Absorption and emission properties of the polymers in $CHCl_3$/film

Polymer	λ_{max}(nm) $CHCl_3$/film	λ_{em}(nm) $CHCl_3$/film	Φ_{PL}(%) $CHCl_3$/film
P1	520/532	590/623	30/7.8
P2	532/555	613/676	11/5.3

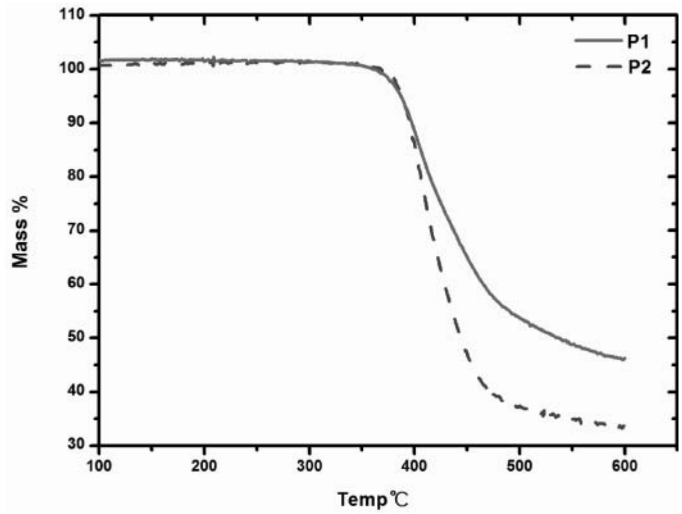

Fig. 3. TGA spectra of **P1** and **P2**.

532 nm, which were the characteristic $\pi \rightarrow \pi^*$ absorption of DPP unit. The red shift of the maximum absorption of **P2** relative to **P1** could be assigned to intramolecular charge transfer (ICT) arisen from the presence of the electron rich 1, 4-octyloxy-2,5-dibenzyl and electron accepting DPP segment (35). Both polymers had a wide absorption wavelength range from 300 to 600 nm, which might be useful for photovoltaic cells (36, 37). Figure 6 shows the absorption spectra of **P1** and **P2** in the film, the maximum absorption of **P2** (555 nm) was similar with that of PDPP-DOPV (553 nm) (33) which was synthesized through Heck polycondensation, indicating that 4-octyloxybenzyl did not have much influence on the absorption properties of the polymer backbone. Like most of the conjugated polymers, the absorption peaks will be red shifted from solution state to film because of molecular aggregation.

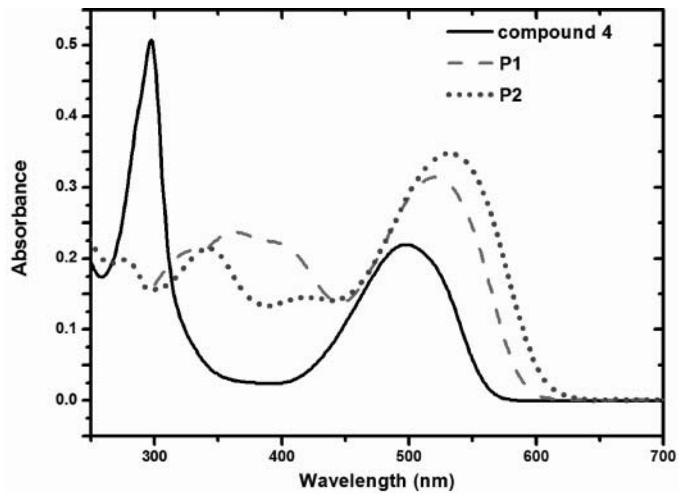

Fig. 4. Absorption spectra of monomer and polymers in dilute $CHCl_3$.

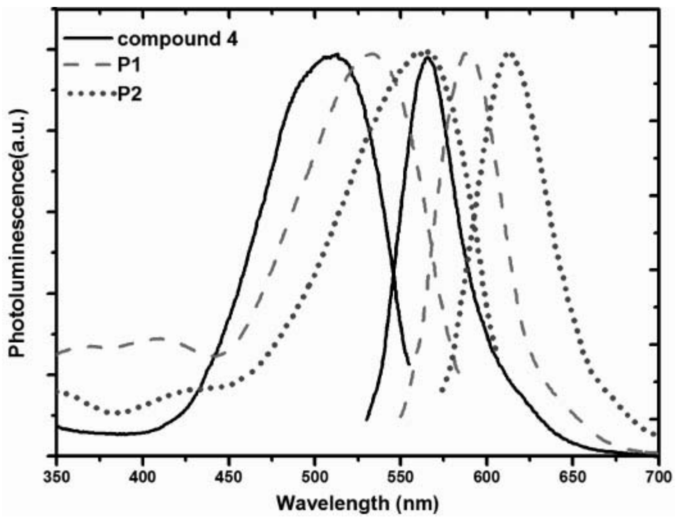

Fig. 5. Excitation and emission spectra of monomer and polymers in dilute $CHCl_3$.

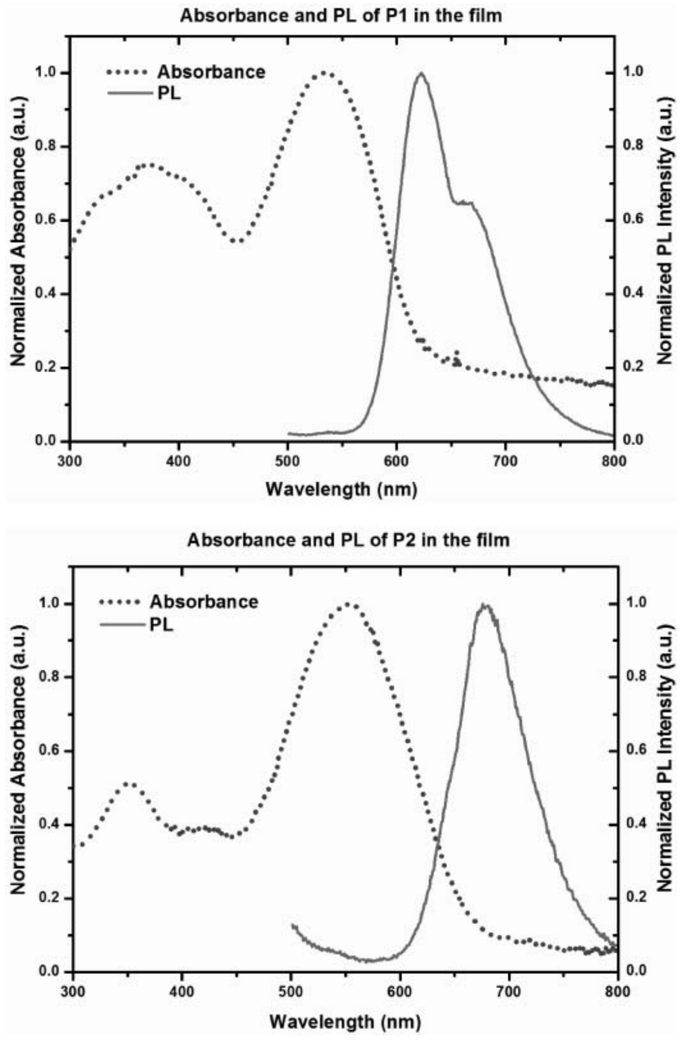

Fig. 6. Absorption and PL of **P1** (top) and **P2** (bottom) in the film.

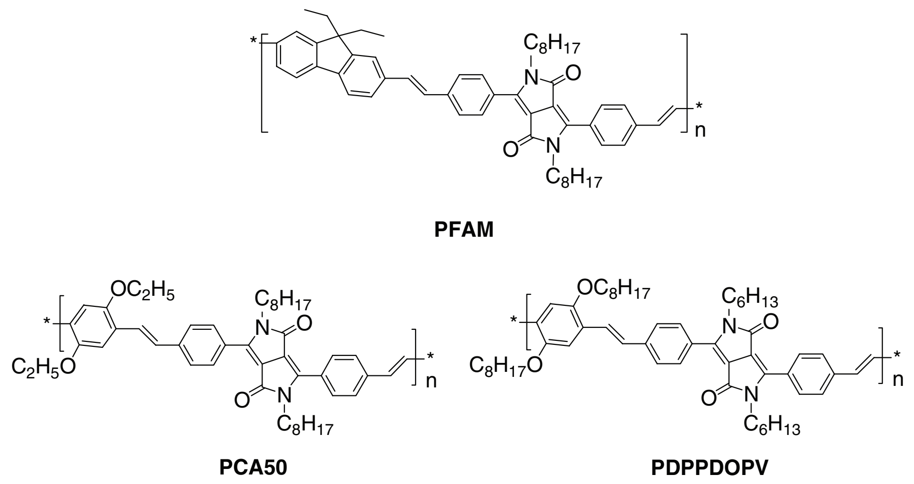

Sch. 2. Structures of PFAM, PCA 50 and PDPPDOPV.

Figure 5 presents the excitation and emission spectra of monomer and polymers in dilute $CHCl_3$ solution (10^{-5} M). The maximum emissions (λ_{em}) of **P1** and **P2** were red shifted relative to the compound **4** (565 nm) as the π-conjugated extension. Figure 5 shows the emission spectra of **P1** and **P2**. Compared to the dilute solution emission spectra, the thin film spectra were red shifted by 33 nm and 63 nm respectively and were broader, probably due to the intermolecular interaction between adjacent polymer chains which increased the ground state energy (38). The red shift of **P2** was larger than that of **P1**. This might due to the stronger ICT of **P2**, which lowers the excitation energy (33, 38). Correspondingly, the PL quantum yields of **P2** both in solution and film states were lower than those of **P1** as ICT quenched fluorescence (39). Benefitting from 4-octyloxybenzyl which could reduce the solid aggregation, the film state PL quantum yield (Φ_{PL}) of both polymers were higher than PFAM (2.58%) (28) and PCA50 (2.56%) (28) with octyl as the side group (Sch. 2). Bulky side group and irregular polymer chain made maximum PL emission of **P2** blue shift relative to the PDPPDOPV (Sch. 2) which was all-trans configuration (33) in solution (10 nm) and especially in film (50 nm).

3.3 Electrochemical Characteristics

The electrochemical properties of the polymers were studied using cyclic voltammetry (CV). Oxidative and reductive cycles of **P1** and **P2** are shown in Figure 7, and CV data are compiled in Table 3. HOMO and LUMO value were calculated according to the equation (40): $E_{\mathrm{HOMO}} = -(E_{\mathrm{onset,ox}} + 4.4)$ eV, $E_{\mathrm{LUMO}} = -(E_{\mathrm{onset,red}} + 4.4)$ eV, where $E_{\mathrm{onset,ox}}$, $E_{\mathrm{onset,red}}$ were the onset potentials for oxidation and reduction process of polymer thin films *vs* SCE. **P1** and **P2** possessed a reversible reduction peak and an irreversible oxidation peak. Polymer film degraded under higher potential during the oxidation process. The band gaps (E_g) of **P1** and **P2** agreed very well with optical band gaps ($E_{g,\mathrm{opt}}$). $E_{\mathrm{gopt}} = 1240/\lambda_{\mathrm{onset}}$ eV, where λ_{onset} is the absorption onsets of UV-vis spectra of the polymer film (613 nm and 656 nm for **P1** and **P2**, respectively). The low LUMO energy level and reversible reduction of the polymers indicated that they had high electron affinity and good electron-transporting ability (12).

Table 3. Electrochemical Potentials and Energy Levels of the Polymers

Polymer	$E_g/E_{g,opt}$ *(eV)*	*Oxidation Onset (V) /HOMO (eV)*	*Reduction Onset (V) /LUMO (eV)*
P1	1.93/2.02	1.14/−5.54	−0.79/−3.61
P2	1.86/1.89	0.98/−5.38	−0.88/−3.52

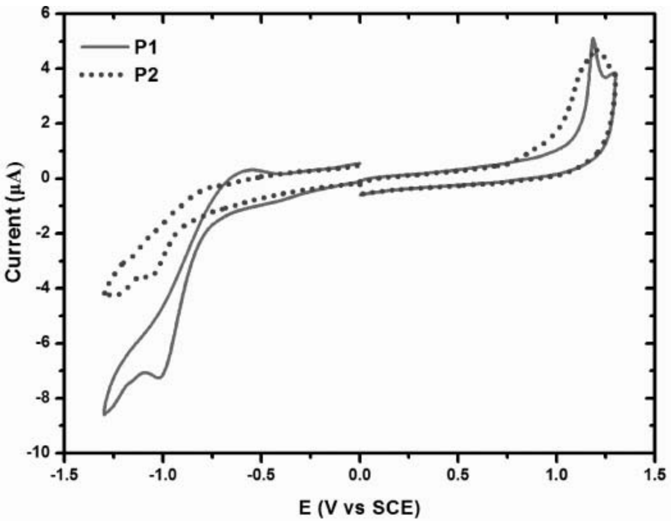

Fig. 7. Cyclic voltammograms of **P1** and **P2** on a Pt electrode at a scanning rate of 50 mV/s.

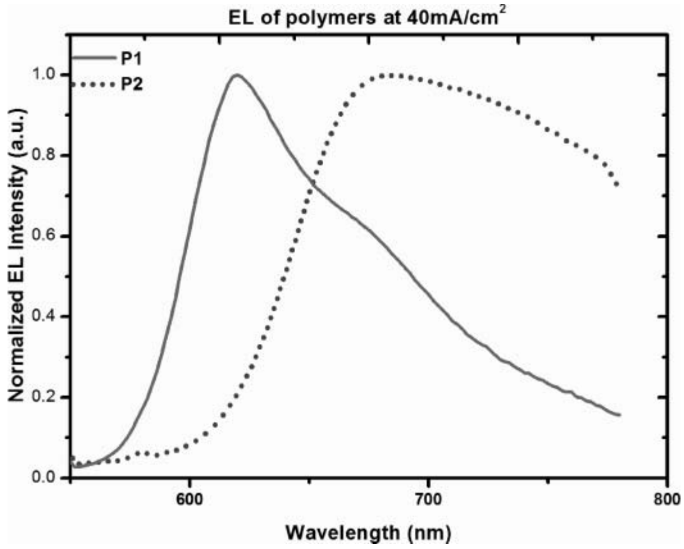

Fig. 8. EL emission spectra of ITO/PEDOT/polymer/CsF/Al.

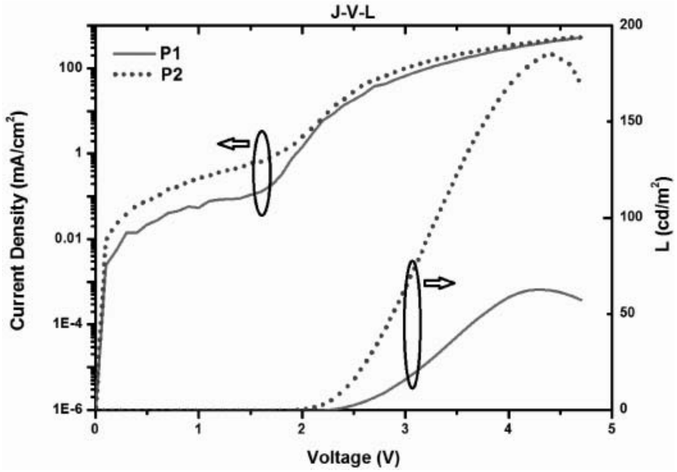

Fig. 9. Current-Voltage and Luminance-Voltage curve of ITO/PEDOT/polymer/CsF/Al.

Compared with PFV and poly(1,4-(2,5-dihexyloxy)-phenylenevinylene-*alt*-1,4- phenylenevinylene) (41) (LUMO levels are about -2.74 eV and -2.86 eV, respectively), the LUMO levels of **P1** and **P2** decreased, indicating that DPP units could reduce the LUMO level of the polymer which was helpful to lower the energy barrier between the polymer and cathode. Comparing with **P1**, the introduction of 1,4-dioctyloxybenzene raised the HOMO energy level in **P2**, and could lower the interface energy barrier between the polymer and PEDOT:PSS (−5.0 eV), indicating that holes could be more easily injected into **P2** than into **P1** in the light emitting diode (42). The work function of CsF/Al is about −1.9 eV (43) which is higher than the LUMO energy levels of **P1** and **P2**, indicating that electrons could easily inject into the polymer.

3.4 Electroluminescence Properties of LEDs

Double-layer device was fabricated in the figuration of ITO/PEDOT/Polymers/CsF/Al, in which PEDOT doped with PSS was used to enhance hole injection/transport and as a buffer layer (12). All obtained devices emit in the red region, the performance of the devices are summarized in Table 4. Figure 8 shows the EL spectra of the devices of **P1** and **P2**. Comparedwith the PL spectra, the EL spectra of the two polymers became broad and extended to long wavelength. This might be attributed to the cross-recombination between electrons in a main chain segment and a hole in nearby electron rich side group 4-octyloxybenzyl, which resulted in lower energy long wavelength emission (44).

The turn-on voltages of the two devices were 2.4 V (P1) and 2.1 V (P2) at 1.5 cd/m^2, which were lower than that of the reported DPP-containing polymers (12,13). Light emission at low turn voltage is necessary since high operating voltage will shorten the device lifetime due to thermal aging and impurity diffusion under high-electric field (25). Like most of DPP alternating copolymers, **P1** and **P2** possessed low LUMO level, and there was almost no energy barrier between the polymer and CsF/Al electrode. There existed a low energy barrier between the polymer and ITO/PEDOT electrode (0.54 eV for P1, 0.38 eV for P2). Therefore, the low turn-on voltages might arise from the lower energy barrier between the emitting layer and electrodes, which led to charge injection easier (45,46). The turn on voltage of the device of **P2** was lower than **P1** because it possibly possessed a lower energy barrier. The current-density plots (Fig. 9) revealed that, at a fixed voltage, a much higher current density was observed for **P2** compared with **P1**. This could be a consequence of the absence of electron-donating comonomer units in **P1** which amplified the hole transport in **P2** (47).

The maximum external quantum efficiencies (EQE) of **P2** was higher than that of **P1**, because it had electron rich 1,4-dioctyloxybenzene in the polymer backbone, which might enhance the hole-transporting to make more

Table 4. Performance of the ITO/PEDOT/polymer/CsF/Al

Polymer	*Maximum EL emission (nm)*	*CIE coordinate (x, y)*	*Turn-on voltage (V)*	*Maximum EQE (%)*	*Maximum brightness (cd/m^2)*
P1	620	(0.63, 0.34)	2.4	0.031	63
P2	682	(0.55, 0.31)	2.1	0.078	186

charge balance (48). In general, the EL external efficiency $\eta_{EL=}\gamma \cdot \eta_{PL} \cdot \eta_C \cdot \chi_S$, where γ relates to the charge balance in the emissive layer, η_{PL} is the photoluminescence quantum efficiency of the emitter, η_C is the fraction of photos coupled out of the device, and χ_S is the singlet fraction. Control of the charge balance γ is an important factor in improving device efficiencies (2). Therefore, the external quantum efficiency of **P2** was higher than that of **P1**, though its PL quantum yield was lower.

4 Conclusions

Two novel DPP-based alternating copolymers with 4-octyloxybenzyl side group were synthesized via Wittig polymerization with good yields. Both polymers have been used as emitting layer in light emitting diodes without much optimization, exhibiting red emission with EL maximum wavelengths at 620 nm (**P1**) and 682 nm (**P2**). The maximum brightness of the devices were 63 cd/m^2 (**P1**) and 186 cd/m^2 (**P2**); the maximum external quantum efficiencies of the devices were 0.031% (**P1**) and 0.078% (**P2**). DPP reduced the LUMO level of the polymer, and the energy barrier between the polymers and electrode was low. Both diodes possessed low turn on voltage (2.4 V and 2.1 V), which was an advantage for PLED. Compared with PFAM and PCA 50 with octyl as the side group, 4-octyloxybenzyl as side group improved the PL quantum yield in thin film, which was due to bulky group reduced the aggregation of polymer chains. **P2** exhibited stronger ICT than **P1**, because it possessed electron rich 1,4-dioctyloxybenzene in the main chain. Thus, the maximum emission wavelength was longer but the PL quantum yield was lower. However, EL performance of **P2** was better than **P1**. It seems that 1,4-dioctyloxybenzene of **P2** possibly enhanced the hole-transporting to make more charge balance which improved the EL performance.

Acknowledgments

This work was supported by the National Natural Science Foundation of China (20872038), Science and Technology Planning Project of Guangdong Province, China (2007A010500011).

References

1. Burroughes, J.H., Bradley, D.D.C., Brown, A.R., Marks, R.N., Mackay, K., Friend, R.H., Burns, P.L. and Holmes, A.B. (1990) *Nature*, 347(6293), 539–541.
2. Grimsdale, A.C., Chan, K.L., Martin, R.E., Jokisz, P.G. and Holmes, A.B. (2009) *Chem. Rev*., 109(3), 897–1091.
3. Chan, L.H., Lee, Y.D. and Chen, C.T. (2006) *Macromolecules*, 39(9), 3262–3269.
4. Yang, J., Jiang, C.Y., Zhang, Y., Yang, R.Q., Yang, W., Hou, Q. and Cao, Y. (2004) *Macromolecules*, 37(4), 1211–1218.
5. Liu, J., Chen, L., Shao, S.Y., Xie, Z.Y., Cheng, Y.X., Geng, Y.H., Wang, L.X., Jing, X.B. and Wang, F.S. (2008) *J. Mater. Chem.*, 18(3), 319–327.
6. Chan, W.K., Chen, Y.M., Peng, Z.H. and Yu, L.P. (1993) *J. Am. Chem. Soc*., 115(25), 11735–11743.
7. Fukuda, M., Kodama, K., Yamamoto, H. and Mito, K. (2004) *Dyes Pigm*., 63(2), 115–125.
8. Zou, Y.P., Gendron, D., Badrou-Aich, R., Najari, A., Tao, Y. and Leclerc, M. (2009) *Macromolecules,* 42(8), 2891–2894.
9. Zhou, E.J., Yamakawa, S.P., Tajima, K., Yang, C.H. and Hashimoto, K. (2009) *Chem. Mater.,* 21(17), 4055–4061.
10. Walker, B., Tomayo, A.B., Dang, X.D., Zalar, P., Seo, J.H., Garcia, A., Tantiwiwat, M. and Nguyen, T.Q. (2009) *Adv. Funct. Mater.,* 19(19), 3063–3069.
11. Bijleveld, J.C., Zoombelt, A.P., Mathijssen, S.G.J., Wienk, M.M., Turbiez, M., de Leeuw, D.M. and Janssen, R.A.J. (2009) *J. Am. Chem. Soc.,* 131(46), 16616–16617.
12. Cao, D.R., Liu, Q.L., Zeng, W.J., Han, S.H., Peng, J.B. and Liu, S.P. (2006) *J. Polym. Sci., Part A: Polym. Chem*., 44(8), 2395–2405.
13. Cao, D.R., Liu, Q.L., Zeng, W.J., Han, S.H., Peng, J.B. and Liu, S.P. (2006) *Macromolecules*, 39(24), 8347–8355.
14. Beyerlein, T., Tieke, B., Forero-Lenger, S. and Brutting, W. (2002) *Synth. Met*., 130(2), 115–119.
15. Zhu, Y., Rabindranath, A.R., Beyerlein, T. and Tieke, B. (2007) *Macromolecules*, 40, 6981–6989.
16. Zhang, K. and Tieke, B. (2008) *Macromolecules*, 41(20), 7287–7295.
17. Rabindranath, A.R., Zhu, Y., Zhang, K. and Tieke, B. (2009) *Polymer*, 50(7), 1637–1644.
18. Wallquist, O. and Lenz, R. (2002) *Macromol. Symp*., 187, 617–629.
19. Tamayo, A.B., Tantiwiwat, M., Walker, B. and Nguyen, T.Q. (2008) *J. Phys. Chem. C*, 112(39), 15543–15552.
20. Huo, L. J., Hou, J. H., Chen, H. Y., Zhang, S. Q., Jiang, Y., Chen, T. L. and Yang, Y. (2009) *Macromolecules*, 42(17), 6564–6571.
21. Chin-Ti, C. (2004) *Chem. Mater*., 16(23), 4389–4400.
22. Chih-Long, C., Min-Fei, W., De-Chang, D., Yuh-Sheng, W., Juen-Kai, W. and Chin-Ti, C. (2005) *Adv. Funct. Mater.,* 15(2), 231–238.
23. Colonna, G., Pilati, T., Rusconi, F. and Zecchi, G. (2007) *Dyes Pigm.,* 75(1), 125–129.
24. Ozdemir, T., Atilgan, S., Kutuk, I., Yildirim, L.T., Tulek, A., Bayindir, M. and Akkaya, E.U. (2009) *Org. Lett*., 11(10), 2105–2107.
25. Madhwal, D., Rait, S.S., Verma, A., Kumar, A., Bhatnagar, P.K., Mathur, P.C. and Onoda, M. (2010) *J. Lumin*., 130(2), 331–333.
26. Tsai, L.R. and Chen, Y. (2008) *Macromolecules*, 41(14), 5098–5106.
27. Li, B., Miao, W.R. and Cheng, L.B. (1999) *Dyes Pigm*., 43(3), 161–165.
28. Qiao, Z. (2009) PhD. Dissertation, South China University of Technology, Guangzhou, China
29. Xia, A.Y., Yuan, Z.L., Tan, S.T., Zou, Y.P., Tan, Z.N., Yang, Y. and Li, Y.F. (2007) *Eur. Polym. J.,* 43(4), 1394–1401.
30. Yang, L.Y., Wang, C., Li, L.Q., Janietz, S., Wedel, A., Hua, Y.L. and Yin, S.G. (2007) *J. Polym. Sci., Part A: Polym. Chem*., 45, 4291–4299.
31. Hasegawa, J., Hamada, M., Miyamoto, T., Nishide, K., Kajimoto, T., Uenishi, J. and Node, M. (2005) *Carbohydr. Res*., 340(15), 2360–2368.
32. Wang, F.F., He, F., Xie, Z.Q., Li, Y.P., Hanif, M., Li, M. and Ma, Y.G. (2008) *Macromol. Chem. Phys.,* 209(13), 1381–1388.
33. Liu, K., Li, Y. and Yang, M.J. (2009) *J. Appl. Polym. Sci*., 111(4), 1976–1984.
34. Mikroyannidis, J.A., Gibbons, K.M., Kulkarni, A.P. and Jenekhe, S.A. (2008) *Macromolecules*, 41(3), 663–674.
35. Mikroyannidis, J.A., Fakis, M. and Spiliopoulos, I.K. (2009) J. *Polym. Sci., Part A: Polym. Chem*., 47(13), 3370–3379.
36. Tao, S., Fute, Z., Xiaojuan, S., Xiaohong, Z., Xiulin, Z. and Baoquan, S. (2009) *Appl. Phys. Lett*., 233502.

37. Brabec, C.J., Winder, C., Sariciftci, N.S., Hummelen, J.C., Dhanabalan, A., van Hal, P.A. and Janssen, R.A.J. (2002) *Adv. Funct. Mater.,* 12(10), 709–712.
38. Zhu, Y., Heim, I. and Tieke, B. (2006) *Macromol. Chem. Phys*., 207, 2206–2214.
39. Chiang, C.L., Tseng, S.M., Chen, C.T., Hsu, C.P. and Shu, C.F. (2008) *Adv. Funct. Mater*., 18(2), 248–257.
40. Cervini, R., Li, X.C., Spencer, G.W.C., Holmes, A.B., Moratti, S.C. and Friend, R.H. (1997) *Synth. Met*., 84(1–3), 359–360.
41. Tsai, C.J. and Chen, Y. (2006) *React. Funct. Polym.,* 66(11), 1327–1335.
42. Sung-Ho, J., Mi-Yeon, K., Dae-Sung, K., Young-Inn, K., Sung-Heum, P., Kwanghee, L. and Yeong-Soon, G. (2004) *Chem. Mater*.,16(17), 3299–3307.
43. Piromreun, P., Oh, H., Shen, Y.L., Malliaras, G.G., Scott, J.C. and Brock, P.J. (2000) *Appl. Phys. Lett*., 77(15), 2403–2405.
44. Jin Long, L., Xiwen, C., Ching Yang, L., Show An, C. and Chiu Huen, S. (2007) *J. Phys. Chem. B*, 10379–10385.
45. Cho, J.H., Lee, H.S., Jang, Y., Lee, Y., Kwon, S.K., Jang, J. and Cho, K. (2006) *Appl. Phys. Lett*., 89(8), 083508.
46. Vak, D., Shin, S.J., Yum, J.H., Kim, S.S. and Kim, D.Y. (2005) *J. Lumin*., 115(3–4), 109–116.
47. Grisorio, R., Piliego, C., Fini, P., Cosma, P., Mastrorilli, P., Gigli, G., Suranna, G.P. and Nobile, C.F. (2008) *J. Polym. Sci., Part A: Polym. Chem*., 46(18), 6051–6063.
48. Herguch, P., Jiang, X.Z., Liu, M.S. and Jen, A.K.Y. (2002) *Macromolecules*, 35(16), 6094–6100.